European Journal of Medicinal Chemistry 46 (2011) 4820–4826

Contents lists available at ScienceDirect

European Journal of Medicinal Chemistry

journal homepage: http://www.elsevier.com/locate/ejmech

Original article

Synthesis, stereochemistry and SAR of a series of minodronate analogues as RGGT inhibitors

Katarzyna M. Błażewska [a,b], Feng Ni [a], Ralf Haiges [a], Boris A. Kashemirov [a], Fraser P. Coxon [c], Charlotte A. Stewart [c], Rudi Baron [d], Michael J. Rogers [c], Miguel C. Seabra [d], Frank H. Ebetino [e], Charles E. McKenna [a,*]

[a] Department of Chemistry, University of Southern California, Los Angeles, CA 90089-0744, USA
[b] Institute of Organic Chemistry, Technical Unversity of Łódź, Zeromskiego St. 116, 90-924 Łódź, Poland
[c] Bone & Musculoskeletal Programme, Institute of Medical Sciences, University of Aberdeen, Aberdeen AB25 2ZD, UK
[d] Molecular Medicine, National Heart and Lung Institute, Imperial College London, London SW7 2AZ, UK
[e] Warner Chilcott Pharmaceuticals, Dundalk, Ireland

ARTICLE INFO

Article history:
Received 26 February 2011
Received in revised form
26 April 2011
Accepted 27 April 2011
Available online 7 May 2011

Keywords:
Phosphonocarboxylates
Bisphosphonates
RGGT inhibitors
X-ray crystallography
Absolute configuration
ee determination

ABSTRACT

Phosphonocarboxylate (PC) analogues of bisphosphonates are of interest due to their selective inhibition of a key enzyme in the mevalonate pathway, Rab geranylgeranyl transferase (RGGT). The dextrarotatory enantiomer of 2-hydroxy-3-(imidazo[1,2-a]pyridin-3-yl)-2-phosphonopropanoic acid (3-IPEHPC, **1**) is the most potent PC-type RGGT inhibitor thus far identified. The absolute configuration of (+)-**1** in the active site complex has remained unknown due to difficulties in obtaining RGGT inhibitor complex crystals suitable for X-ray diffraction analysis. However, we have now succeeded in crystallizing (−)-**1** and here report its absolute configuration (AC) obtained by X-ray crystallography, thus also defining the AC of (+)-**1**. An Autodock Vina 1.1 computer modeling study of (+)-**1** in the active site of modified RGGT binding GGPP (3DSV) identifies stereochemistry-dependent interactions that could account for the potency of (+)-**1** and supports the hypothesis that this type of inhibitor binds at the TAG tunnel, inhibiting the second geranylgeranylation step. We also report a convenient ^{31}P NMR method to determine enantiomeric excess of **1** and its pyridyl analogue **2**, using α- and β-cyclodextrins as chiral solvating agents, and describe the synthesis of a small series of **1** α-*X* (*X* = H, F, Cl, Br; **7a**–**d**) analogues to assess the contribution of the α-OH group to activity at enzyme and cellular levels. The IC_{50} of **1** was 5 −10× lower than **7a**–**d**, and the LED for inhibition of Rab11 prenylation *in vitro* was 2–8× lower than for **7a**–**d**. However, in a viability reduction assay with J774 cells, **1** and **7b** had similar IC_{50} values, ~10× lower than those of **7a** and **7c**–**d**.

1. Introduction

2-hydroxy-3-(imidazo[1,2-a]pyridin-3-yl)-2-phosphonopropanoic acid (3-IPEHPC, **1**) [1,2] and 2-hydroxy-2-phosphono-3-(pyridin-3-yl)propanoic acid (3-PEHPC, **2**) [3] are phosphonocarboxylate (PC) analogues of two clinical heterocyclic bisphosphonate (BP) drugs, minodronic and risedronic acids, that block prenylation by inhibiting a mevalonate pathway enzyme, FPPS [4]. In PC analogues, one phosphonic acid group of the BP is replaced by a carboxylic acid group, creating a chiral center at the α-carbon. In general, PCs exhibit lower bone affinity than the BPs but retain some ability to block protein prenylation [5] by inhibiting a downstream mevalonate pathway enzyme, Rab geranylgeranyl transferase (RabGGTase, RGGT), thus selectively preventing prenylation of Rab family GTPases [3,6]. Rab proteins are responsible for a broad range of intracellular trafficking events and some were found to contribute to the aggressiveness and progression of various cancers [7]. **2** has shown anti-tumour activity *in vitro* [8,9] and also in an animal model [10]. PC derivatives have proven useful as tools for investigating Rab-dependent biological processes [11], as well as in bone distribution studies [12] (Fig. 1).

RGGT is responsible for transferring two geranylgeranyl (GG) groups to Rab proteins. There is evidence that PCs prevent only the second GG transfer to Rab proteins, showing uncompetitive inhibition against Rab proteins and mixed-type inhibition against geranylgeranyl pyrophosphate (GGPP) [1]. This differentiates them

* Corresponding author.
E-mail address: mckenna@usc.edu (C.E. McKenna).

0223-5234/$ – see front matter © 2011 Elsevier Masson SAS. All rights reserved.
doi:10.1016/j.ejmech.2011.04.063

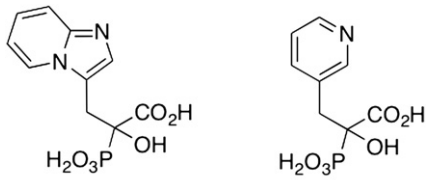

Fig. 1. Phosphonocarboxylic acids 3-IPEHPC (**1**) and 3-PEHPC (**2**).

from other RGGT inhibitors, and suggests that they target a different part of the active site [1]. A crystal structure for the complex of an engineered form of RGGT lacking LRR and Ig-domains with the peptide-based inhibitor is now available [13], but information concerning the second prenylation step is sparse [14], limiting rational design of more potent inhibitors derived from phosphonocarboxylates. On the basis of the crystal structure, a "TAG tunnel" motif has been proposed to play an important role in the binding of selective inhibitors of the second prenylation step [13], and this mechanistic hypothesis is currently being explored [1,14].

Phosphonocarboxylates have not been systematically investigated as RGGT inhibitors, but among a small array of **2** derivatives, in which α-OH was replaced with a hydrogen or halogen substituent [2,5], four proved to be RGGT inhibitors at low micromolar concentrations, placing them among the more active RGGT inhibitors known so far. As **1** is significantly more potent than **2**, it was also of interest to examine the contribution of its α-OH group to its activity [15].

2. Synthesis

We prepared a series of **1** derivatives in which the α-hydroxyl group was replaced by a hydrogen or halogen atom, allowing a comparison with the **2** series to explore the role of the heterocyclic base relative to the α-substituent in determining potency against RGGT. An advantage of the new analogues compared to **1** is their facile synthesis, with the three α-halo-analogues obtained straightforwardly from a common precursor, the α-H analogue **6a** (Scheme 1).

Table 1
Selected ^{31}P and ^{13}C NMR chemical shifts of **6** and **7**.

Compound α-X	**6**[a]		**7**[b]
	^{31}P NMR	^{13}C NMR[c]	^{31}P NMR
H	20.9	44.7 (d, $^1J_{CP}$ = 130.2 Hz)	12.9
F	11.6 (d, $^2J_{PF}$ = 83.9 Hz)	96.9 (dd, $^1J_{CF}$, $^1J_{CP}$ = 202, 159 Hz)	10.1[d] (d, $^2J_{PF}$ = 70.0 Hz)
Cl	14.3	68.5 (d, $^1J_{CP}$ = 144 Hz)	9.68
Br	14.8	57.8 (d, $^1J_{CP}$ = 142 Hz)	9.68

[a] Spectra recorded in $CDCl_3$.
[b] Spectra recorded in D_2O, pH ~2.5.
[c] C_α.
[d] Spectra recorded in D_2O, pH 12.6.

The point of departure was aldehyde **3**, which was converted into alcohol **4** via reduction with $NaBH_4$ in refluxing methanol. After conversion of **4** to chloride **5** by the action of thionyl chloride, excess $SOCl_2$ was evaporated and reaction with the carbanion of triethyl phosphonoacetate gave **6a**, which could be used directly for the synthesis of the desoxy free acid **7a** (see below), or else halogenated with Selectfluor, chlorosuccinimide or bromosuccinimide leading to α-fluoro-, α-chloro- and α-bromo esters **6b**–**d**, respectively, in yields ranging from 18 to 93%. The α-fluoro- and α-chloro esters (**6b** and **6c**) were purified by $NaHCO_3$ (aq) washing and preparative TLC. The α-bromo analogue **6d** could be completely purified by washing with acetone and ethanol only after hydrolysis into the free acid. The esters **6a**–**d** were hydrolyzed by refluxing in concentrated HCl to give the free acids **7a**–**d**, isolated in 58–86% yield. The esters were characterized by ^{31}P, ^1H, ^{13}C NMR spectroscopy and by HRMS. The free acids were characterized by ^{31}P, ^1H NMR and elemental analysis. Selected ^{31}P and ^{13}C NMR chemical shifts for the esters and free acids are presented in Table 1.

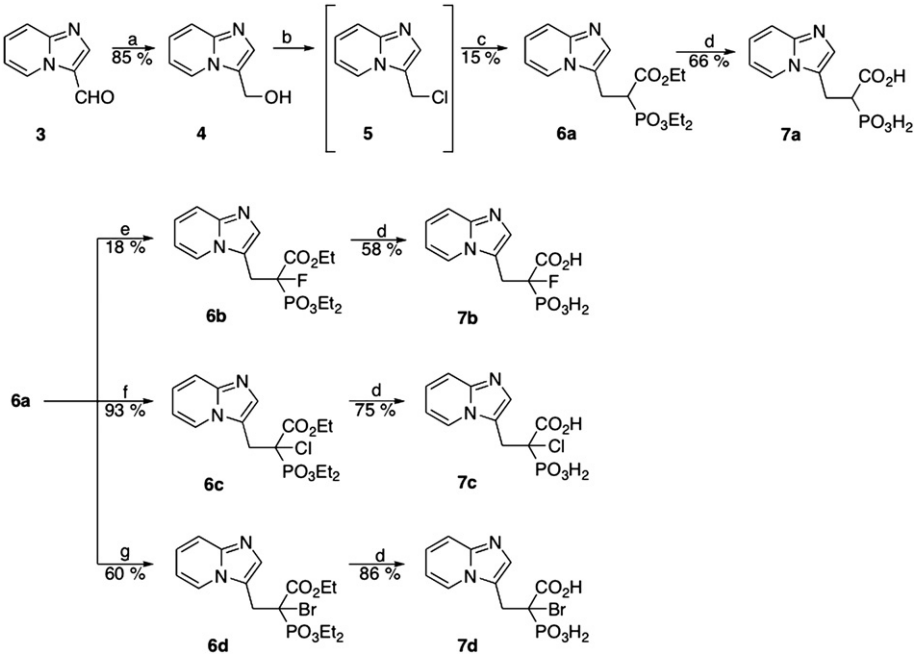

Scheme 1. Reagents and conditions: (a) $NaBH_4$, MeOH, reflux; (b) $SOCl_2$, reflux; (c) triethyl phosphonoacetate, NaH, DMF, THF, 0° to RT; (d) 12 M HCl, reflux; (e) Selectfluor, NaH, THF; (f) *N*-chlorosuccinimide, NaH, THF; (g) *N*-bromosuccinimide, NaH, THF.

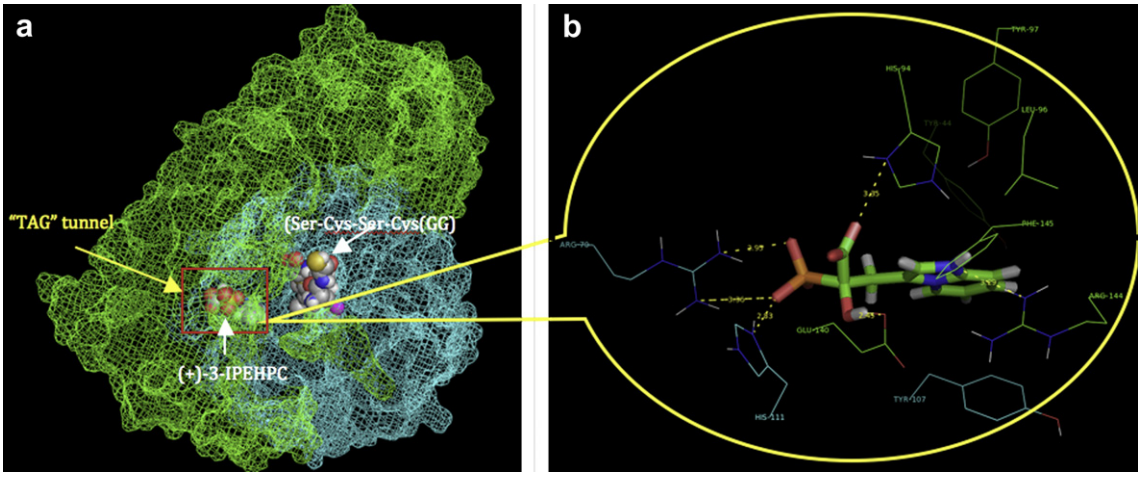

Fig. 2. a) Left:Structure of docked (+)-**1** in RGGT/Ser–Cys–Ser–Cys(GG) complex. (subunit A (green mesh), subunit B (cyan mesh), (+)-**1** and Ser–Cys–Ser–Cys(GG) (sphere)). b) Right: Interactions between (+)-**1** and "TAG" tunnel. ((+)-**1** (stick), protein residue (line)). (For interpretation of the references to colour in this figure legend, the reader is referred to the web version of this article.)

3. Absolute configuration of (+)-1 and its RGGT binding interaction from modeling

Given the importance of stereochemistry in the interaction of **1** with RGGT the absolute configuration (AC) of the more potent enantiomer is essential information, but no crystal structure of PC inhibitor bound to RGGT has yet been obtained. We succeeded in obtaining a crystal of (−)-**1** suitable for X-ray diffraction structural analysis by slow evaporation of an aqueous solution of the pure enantiomer in the presence of acetone vapour at room temperature. The crystallographic structure revealed that the (−)-**1** enantiomer has (*R*) configuration at the α-C (Fig. 3), and therefore the AC of the more potent (+)-**1** enantiomer must be (*S*).

Previous work showed that PCs such as **1** and **2** give mixed-type inhibition with GGPP when inhibiting the second geranylgeranylation (GG) of Rab protein by RGGT, implying that **1** and **2** may bind to a site different from the GGPP binding pocket [1]. We virtually docked (+)-**1** into the active site of monogeranylgeranylated peptide-bound rat RGGT (which is 91.4% and 95.8% homologous to chain A and chain B of human RGGT, respectively) [14] using two software packages: Autodock Vina 1.1 [16] and Dock 6.3 [17]. The results show that (+)-**1** preferentially binds to a site within the "TAG" tunnel [13] (Fig. 2a), which is close to the site where the mono GG-cysteine complex forms and has been proposed as the location where the first GG-cysteine is translocated [13,18]. Interactions between (+)-**1** and the protein potentially involve one ionic H-bond between the hydroxy group of (+)-**1** and the carboxylate of GLU140, salt bridges between the phosphonate and ARG70/HIS111, a salt bridge between the carboxylate of (+)-**1** and HIS94, and immersion of the imidazo[1,2-a]pyridine heterocycle in a hydrophobic pocket formed from TYR44, LEU96, TYR97, TYR107 and PHE145 (Fig. 2b).

Interestingly, although a completely different enzyme is involved, a similar mechanism has been proposed to explain the interactions of risedronate (K_i = 0.36 nmol) and minodronate (K_i = 0.0005 nmol) with FPPS, which also has a hydrophobic pocket constructed chiefly from aromatic amino acid residues [19].

4. NMR analysis of PC chirality aided by cyclodextrin complexes

In view of the profound effect of **1** chirality on RGGT inhibition, we sought a method for fast and accurate ee assignment of such heterocyclic PC compounds. Initially, we used chiral HPLC to determine ee by separating the enantiomers chromatographically, but due to peak tailing this method is not ideal for precise ee assignment. The measured ee values varied, depending on the column chirality (Fig. 4a).

We then investigated the application of cyclodextrins as chiral solvating agents to assign the ee of phosphonocarboxylate enantiomers by ^{31}P NMR. NMR spectroscopy is one of the most commonly used techniques for the assignment of enantiomeric purity and absolute configuration of different classes of chiral compounds [20–22]. Enantiomers can be differentiated either by forming a new covalent bond with a chiral derivatizing agent (CDA), or by the addition of a chiral solvating agent (CSA), to form a diastereomeric complex. Enantiomeric α-aminophosphonic acids have been analyzed by ^{31}P {^{1}H} NMR [23–25]. In this work we found that acquisition of a ^{31}P {^{1}H} NMR spectrum of racemic phosphonocarboxylate mixed with the appropriate cyclodextrin in D_2O solution, pH 9.5 gave two signals with baseline peak resolution (Table 2), enabling ee determination to the accuracy and precision of the NMR peak integration, including samples of ~100% ee (Fig. 4b). It can be noted that the average of the two chiral HPLC determinations for ee of the sample with <100% ee ((−)-**1**) equals that obtained by the NMR method (Fig. 4a and 4b, right). The method was successful with both **1** and **2**, but only with a particular

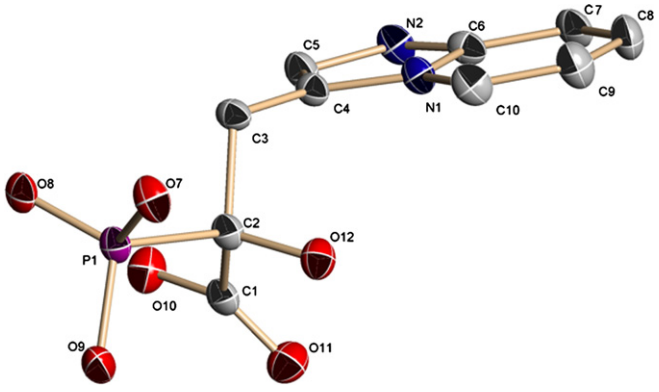

Fig. 3. Molecular structure of (−)-**1** from X-ray crystallographic analysis. The α-C has (*R*) configuration. Thermal ellipsoids are shown at the 50% probability level.

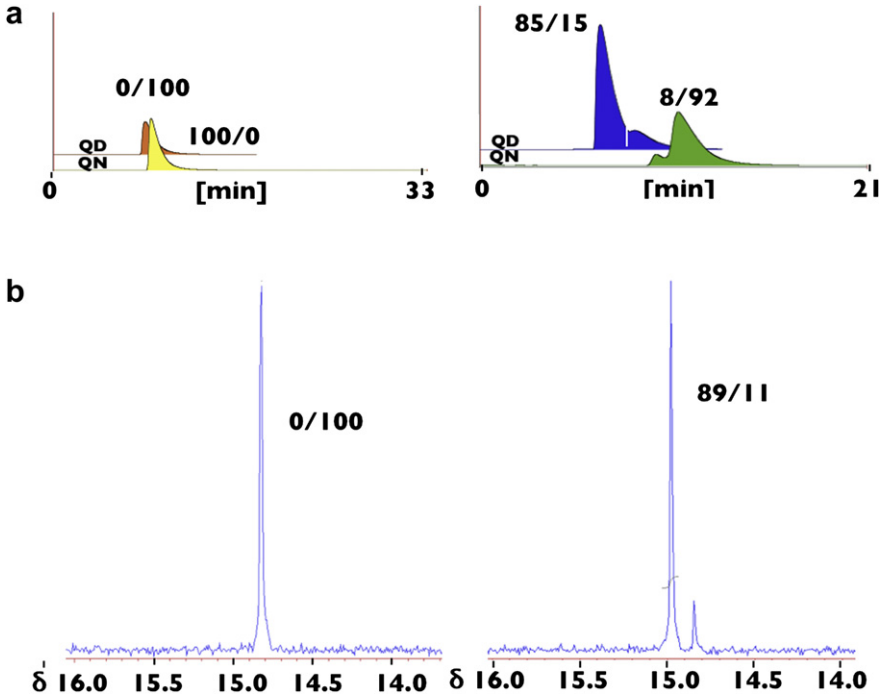

Fig. 4. Determination of ee in resolved and partially resolved samples of **1** after preparative chiral HPLC: a) Left: chiral HPLC analysis of (+)-**1** isolated as the leading peak on a QN chiral HPLC column on a preparative HPLC column of opposite chirality (QN-quinine, QD-quinidine). Right: same analysis of (−)-**1**, isolated as the trailing peak on a preparative QN HPLC column; b) Analysis of the same sample of (+)-**1** (left) and (−)-**1** (right) by ^{31}P NMR using β-CD (D_2O, pH 9.5) as a chiral solvating agent.

CD in each case (Table 2). The 6-membered pyridyl ring of **2** apparently fits better into the smaller cavity of α-CD, whereas the larger imidazo[1,2-a]pyridine ring of **1** is more easily accommodated in the larger cavity available with β-CD. Therefore, for **1** derivatives β-CD was preferentially used, and α-CD for **2** derivatives. The Δδ values also depend on the other PC α-substituent, with values ranging from 0.03 ppm for the desoxy analogue **7a** to 0.67 ppm for the bromo analogue **7d**. With the fluoro derivative **7b**, additional splitting in the ^{31}P NMR was observed due to ^{19}F coupling which masked the baseline separation but the alternative of ^{19}F NMR for the ee determination could be applied ($\Delta\delta = 0.08$ ppm ^{31}P NMR and $\Delta\delta = 0.1$ ppm ^{19}F NMR). Compared to β-CD, use of γ-CD (increased cavity size) gave worse resolution of both **1** and **7d** (with 10 eq of γ-CD the values were $\Delta\delta = 0.012$ ppm and $\Delta\delta = 0$ ppm, respectively). No interference due to residual buffer (AcOH, TEA) from preparative HPLC separation was encountered in the ^{31}P NMR resolutions, which eliminated the need to transfer the enantiomer samples into their free acid form.

Table 2
^{31}P NMR chemical shift nonequivalence (Δδ) found for enantiomers of phosphonocarboxylates (~2.5 mM).

Compound (racemic)	α-CD, ^{31}P NMR Δδ (ppm)	β–CD, ^{31}P NMR Δδ (ppm)
2	0.13[a]	0.061[b]
1	0.062[c]	0.13
7a	0.045	0.03[b]
7b	nd	0.082
7c	0.081	0.379
7d	0.055[b,c]	0.666

[a] 10 eq α-CD.
[b] No baseline separation.
[c] 1.25 mM PC.

Table 3
Effect on J774 cell viability, RGGT inhibition and inhibition of Rab11 prenylation of **7a**–**d** vs. **1**.

Compound	α-X	Reduction of J774 viability (IC_{50}/mM)	RGGT inhibition (IC_{50}/μM)	Inhibition of Rab11 prenylation (LED/μM)
1	OH	0.05	1.24	3
7b	F	0.06	6.11	6
7c	Cl	0.40	7.5	12
7d	Br	>0.60	5.56	25
7a	H	>0.60	13.36	12

5. Structure–activity relationship studies – role of the α-OH substituent

The desoxy and halo analogues of **1** were tested for potency as RGGT inhibitors. All of the derivatives **7a**–**d** were at least ~5 times less potent than **1** itself (IC_{50}) (Table 3). The analogues inhibited Rab prenylation and reduced J774 viability, but again with up to 15-fold lower inhibitory potency `than **1**. While the RGGT inhibitory potencies of **7b**–**d** did not differ significantly (IC_{50} 5.56–7.5 μM), the fluoro analogue **7b** was more active in the cell viability and prenylation assays, with potencies only 1.2–2 times less than **1**. Overall, the α-hydroxyl group has a more profound effect on inhibitor activity than it does in **2**, when comparing the equivalent analogues [5]. Moreover, in contrast to the **2** analogues [5], where the fluoro derivative was slightly more active than **2** itself, **1** remains the most active compound in this series.

6. Conclusions

Firstly, the determination of the absolute configuration of the most potent PC inhibitor of RGGT, **1**, supported by computational results has provided useful insights into the interactions between the inhibitor and the active site of RGGT, including an explanation

for the stereochemical preference of the enzyme for the (+)-**1** enantiomer. Comparison of **1** with its racemic α-desoxy, α-fluoro, α-chloro and α-bromo analogues suggests that the α-hydroxy of **1** contributes to its overall potency as an RGGT inhibitor, which is also reflected at the level of *in vitro* cellular prenylation and, except in the case of **7b** which exhibits similar activity, impairment of cellular viability, providing evidence for the key role of the heterocyclic base, the other α-substituent, on PC potency against RGGT. Secondly, in the presence of an appropriate cyclodextrin, ^{31}P NMR provides a new, more convenient and accurate method of ee assignment of PCs such as **1** or **2**, or **7a**–**d**.

7. Experimental

All reagents were purchased from Sigma–Aldrich. DMF was of DrySolv quality. Phosphorus oxychloride, thionyl chloride and triethyl phosphonoacetate were distilled before use. THF was always freshly distilled from benzophenone-sodium. For halogenation reactions, flasks were flame-dried. Halogenation reactions were run under Ar. NMR spectra were measured on a Varian Mercury 400 spectrometer. Chemical shifts (δ) are reported in parts per million (ppm) relative to internal residual $CHCl_3$ in $CDCl_3$ (δ 7.29, ^{1}H), internal residual HDO in D_2O (pH ~2.5, δ 4.68 ^{1}H), or external H_3PO_4 (δ 0.00, ^{31}P). The final products (free acids, 0.5–1 mg) were dissolved in 0.7 mL D_2O, giving pH ~2.5. NMR sample solutions were heated briefly for complete dissolution. Elemental analysis was performed by Gallbraith Laboratories Inc., Knoxville, TN.

Biological assays: RGGT assays, assessment of effects on protein prenylation and measurement of viable J774 cell number were performed according to literature procedures [5].

Molecular docking: The ligand receptor site is a structure obtained from RGGT in complex with monogeranylgeranylated peptide Ser–Cys–Ser–Cys (GG) derived from Rab7 (PDB code: 3DSV). The coordinates of Ser–Cys–Ser–Cys are missing from the structure, but the coordinates of the GG moiety are clearly determined [14]. The protein residues and C15 moiety were kept rigid during the docking experiments. Ligands were generated by Prodrg Server [26]. Autodock Vina 1 [16] was used as the initial docking tool to generate an inhibitor/enzyme complex using the following settings: center_x = 5, center_y = 15, center_z = 31, size_x = 40, size_y = 40, size_z = 40, exhaustiveness = 20, cpu = 4, num_modes = 20, energy_range = 5. Then the top ranked inhibitors given by Vina were subjected to rescoring by the amber_score module implemented in Dock 6.3 [17] using default settings, generating the energy-minimized final coordinates of the complex for analysis.

7.1. Enantiomeric purity assignment with cyclodextrins

The appropriate phosphonocarboxylate was dissolved in D_2O in an NMR tube and the pH was adjusted to 9.5 with a few microliters of 2.5 M NaOH (concentration of PC ~2.5 mM, volume 0.6 mL). Then α-CD (30 eq) or β-CD (5 eq) was added and the ^{31}P NMR spectrum acquired.

7.2. Imidazo[1,2-a]pyridin-3-carbaldehyde (**3**) [27,28]

To DMF (120 mL, 1.55 mol) at 2 °C, freshly distilled phosphorus oxychloride (61 mL, 0.65 mol) was slowly added. The temperature was allowed to rise gradually to room temperature. The solution was cooled again to 2 °C and a solution of imidazo[1,2-a]-pyridine 1 (10 g, 0.085 mol) in DMF (60 mL) was added dropwise. The mixture was warmed to 105 °C, whereupon the temperature rose to 140 °C. The oil bath was removed until the temperature stabilized at 120 °C. The reaction mixture was heated for 45 min at 120 °C and 2.5 h at 85 °C, then cooled and poured into 5% HCl (600 mL) ice-cooled and brought to pH 9 using 20% NaOH. The resulting solution was extracted with CH_2Cl_2 (1200 mL) overnight. Then the organic layer was separated and dried over $MgSO_4$, the solvent removed under reduced pressure, the crude product washed with water (5 × 15 mL) and again dried, providing the pure product 3.49 g (31%).

7.3. 3-Hydroxymethylimidazo[1,2-a]pyridine (**4**) [28]

Sodium borohydride (1.61 g, 2.1 eq) was added to a solution of aldehyde **3** (2.92 g, 0.02 mol) in 400 mL of MeOH. The homogenous solution was refluxed for 1 h (oil bath, 75 °C). The progress of the reaction was checked either by NMR (evaporation of 1 mL of reaction mixture, dissolution in $CDCl_3$) or by TLC (acetone, R_f(substrate) = 0.56, R_f(product) = 0.24). The reaction mixture was cooled to RT, quenched with 30 mL of 6 N HCl, evaporated to dryness and treated with 70 mL of saturated sodium carbonate solution. The resulting non-homogenous mixture was evaporated to dryness and the semi-solid residue extracted with CH_2Cl_2 (5 × 110 mL), and then for another 2 h with 60 mL of CH_2Cl_2. The combined organic extracts were dried over Na_2SO_4 and evaporated to dryness, giving 2.53 g of product (85.5%).

7.3.1. Ethyl 2-(diethoxyphosphoryl)-3-(imidazo[1,2-a]pyridin-3-yl) propanoate (**6a**)

Alcohol **4** (1.48 g, 0.01 mol) was added to cold (ice bath) thionyl chloride (40 mL, 55 eq) and refluxed for 20 min. Gaseous products and excess $SOCl_2$ were removed in the hood under argon, using water aspirator and then oil vacuum pump (between the pumps and the apparatus, a trap cooled with acetone/dry ice was installed). Then 8 mL of DMF and NaH (0.41 g, 0.017 mol) were added. The mixture was stirred for 0.5 h at RT. In another flask triethyl phosphonoacetate (2.24 g, 0.01 eq) in 4 mL of THF was added dropwise to the cooled mixture of sodium hydride (0.41 g, 0.017 mol) in THF (4 mL). It was stirred on an ice bath for 15 min and then for 45 min at RT. Chloride **5** in DMF was added via a pipette. After 2.5 h the reaction mixture was quenched with acetic acid (0.1 mL) in water (25 mL), pH 6, then extracted with CH_2Cl_2 (4 × 50 mL). After drying over Na_2SO_4, the organic phase was evaporated and the residue subjected to column chromatography (gradient elution: AcOEt to AcOEt:acetone, 1:2). The product **6a** was isolated in 15% yield, 93% purity. ^{1}H NMR ($CDCl_3$): 1.22 (t, $^3J_{HH}$ = 7.20, C(O)OCH$_2$C*H*$_3$, 3H), 1.39 (t, $^3J_{HH}$ = 7.20, P(O)OCH$_2$C*H*$_3$, 3H), 1.40 (t, $^3J_{HH}$ = 7.20, P(O)OCH$_2$C*H*$_3$, 3H), 3.34–3.44 (m, CHHCHP, 2H), 3.65 (ddd, $^2J_{HH}$ = 16.0, $^3J_{HP}$ = 12.0, 7.2, CHHCHP, 1H), 4.11–4.27 (m, OCH$_2$, 6H), 6.88 (dt, $^3J_{HH}$ = 6.4, $^4J_{HH}$ = 0.8, CH, 1H), 7.20 (ddd, $^3J_{HH}$ = 8.8, 6.4, $^4J_{HH}$ = 0.8, CH, 1H), 7.46 (s, CH), 7.61–7.64 (m, CH), 8.08 (bd, $^3J_{HH}$ = 6.4, CH). ^{31}P NMR ($CDCl_3$): 20.94. ^{13}C NMR ($CDCl_3$): 14.45 (s, C(O)OCH$_2$CH$_3$), 16.85 (s, P(O)OCH$_2$CH$_3$, 2C), 22.00 (s, CH$_2$CH), 44.70 (d, $^1J_{CP}$ = 130.2, CHP), 62.30 (s, C(O)OCH$_2$), 63.56 (d, $^2J_{CP}$ = 7.2, P(O)OCH$_2$), 63.67 (d, $^2J_{CP}$ = 5.8, P(O)OCH$_2$), 112.81 (s, CH), 118.37 (s, CH), 121.44 (d, $^3J_{CP}$ = 17.00, C), 123.50 (s, CH), 124.29 (s, CH), 132.09 (s, CH), 146.04 (s, CH), 168.68 (d, $^2J_{CP}$ = 5.85, C=O).

7.3.2. Ethyl 2-chloro-2-(diethoxyphosphoryl)-3-(imidazo[1,2-a] pyridin-3-yl)propanoate (**6c**)

To a cooled mixture of NaH (34 mg, 3 eq) in THF (2.5 mL) a solution of **6a** (0.165 g, 0.47 mmol) was added dropwise, giving a yellow solution, which after stirring for 20 min at 0 °C and 30 min at RT turned brown. It was then cooled to 0 °C and *N*-chlorosuccinimide (0.126 g, 2 eq) was added in one portion. The mixture was kept at 0 °C for 1 h and then at RT overnight. On the following

day, ^{31}P NMR showed completion of the reaction. The reaction was quenched with EtOH (a few drops), diluted with 10 mL CH_2Cl_2 and 5 mL $NaHCO_3$ (aq) up to pH 8–9. After extraction with CH_2Cl_2 (30 mL) by vortex, the organic layers were separated and dried over sodium sulfate and then subjected to prep TLC (CH_2Cl_2:MeOH 16:1). Bands were extracted with MeOH (5 × 10 mL). After the prep TLC residual succinimide remained (^{1}H NMR: 2.8 ppm (s); ^{13}C NMR: ~31 and ~179 ppm). Therefore, a sample of **6c** (31.4 mg) was dissolved in 1.5 mL DCM and vortexed with $NaHCO_3$ (aq) (1 g in 20 mL) 3 times (3 × 0.350 mL), 1 min each extraction. The organic phase was dried, giving pure product (yield 93%). Fluoro-**6b** (18%) and bromo-**6d** (60%) analogues were synthesized similarly, using Selectfluor or bromosuccinimide respectively, instead of chlorosuccinimide.

*7.3.3. Ethyl 2-(diethoxyphosphoryl)-2-fluoro-3-(imidazo[1,2-a] pyridin-3-yl)propanoate (**6b**)*

^{1}H NMR ($CDCl_3$): 1.23 (t, $^3J_{HH}$ = 7.20, C(O)OCH_2CH_3, 3H), 1.39 (t, $^3J_{HH}$ = 7.20, P(O)OCH_2CH_3, 3H), 1.40 (t, $^3J_{HH}$ = 7.20, P(O)OCH_2CH_3, 3H), 3.77 (ddd, $^2J_{HH}$ = 16.00, $^3J_{FH}$ = 12.4, $^3J_{PH}$ = 6.8, C*HH*CHP, 1H), 3.93 (ddd, $^2J_{HH}$ = 16.0, $^3J_{FH}$ = 37.2, $^3J_{PH}$ = 6.0, C*HH*CHP 1H), 4.22–4.35 (m, OCH_2, 6H), 6.86 (dt, $^3J_{HH}$ = 7.2, $^4J_{HH}$ = 0.8, CH, 1H), 7.21 (ddd, $^3J_{HH}$ = 9.2, 7.2, $^4J_{HH}$ = 1.2, CH, 1H), 7.54 (s, CH), 7.62 (dd, $^3J_{HH}$ = 9.2, $^4J_{HH}$ = 0.8, CH), 8.17 (dd, $^3J_{HH}$ = 7.2, $^4J_{HH}$ = 1.2, CH). ^{19}F NMR ($CDCl_3$): −176.31 (bdd, $^2J_{PF}$ = 85.1, $^3J_{FH}$ = 35.8). ^{31}P NMR ($CDCl_3$): 11.56 (d, $^2J_{PF}$ = 83.9). ^{13} C NMR: 14.64 (s, C(O)OCH_2), 17.04, 17.10 (2s, P(O)$(OCH_2CH_3)_2$, 2C), 29.00 (d, $^2J_{CP}$ = 21.1, CH_2C), 63.46 (s, C(O)OCH_2), 65.16 (d, $^2J_{CP}$ = 6.7, P(O)OCH_2), 65.51 (d, $^2J_{CP}$ = 5.2, P(O)OCH_2), 96.90 (dd, $^1J_{CP/CF}$ = 202.0, 159.4, FCP), 112.9 (s, CH), 117.1 (d, *J* = 10.2, C), 118.5 (s, CH), 124.5, 124.8 (s, CH, CH), 134.7 (s, CH), 147.0 (s, CH), 167.0 (d, ^2J = 18.6, C═O). Isolated by preparative TLC (acetone:MeOH 15:1) with 18% yield.

*7.3.4. Ethyl 2-chloro-2-(diethoxyphosphoryl)-3-(imidazo[1,2-a] pyridin-3-yl)propanoate (**6c**)*

^{1}H NMR ($CDCl_3$): 1.30 (t, $^3J_{HH}$ = 7.2, C(O)OCH_2CH_3, 3H), 1.41 (t, $^3J_{HP}$ = 7.2, P(O)OCH_2CH_3, 3H), 1.42 (t, $^3J_{HP}$ = 7.2, P(O)OCH_2CH_3, 3H), 3.79 (dd, $^2J_{HH}$ = 16.0, $^3J_{HP}$ = 8.8, CHHC, 1H), 4.20 (dd, $^2J_{HH}$ = 16.0, $^3J_{HP}$ = 6.0, CHHCH, 1H), 4.23–4.44 (m, 3OCH_2CH_3, 6H), 6.87 (bt, $^3J_{HH}$ = 7.2, CH, 1H), 7.22 (bdd, $^3J_{HH}$ = 9.6, 7.2, CH, 1H), 7.62 (s, CH, 1H), 7.65 (bd, $^3J_{HH}$ = 9.6, CH, 1H), 8.29 (bd, $^3J_{HH}$ = 7.2, CH, 1H). ^{31}P NMR: 14.29. ^{13}C NMR: 14.32 (s, C(O)OCH_2CH_3), 16.86 (s, P(O)$(OCH_2CH_3)_2$, 2C), 30.23 (s, CH_2CP), 64.04 (s, C(O)OCH_2), 65.66 (d, $^3J_{PC}$ = 7.1, P(O)OCH_2), 66.10 (d, $^3J_{PC}$ = 7.0, P(O)OCH_2), 68.50 (d, $^1J_{CP}$ = 144.1, CP), 112.4 (s, CH), 118.2 (s, CH, C, 2C), 124.5 (s, 2CH), 134.8 (s, CH), 146.2 (s, CH), 166.6 (s, 166.6, C═O). Isolated by preparative TLC (DCM:MeOH 16:1).

*7.3.5. Ethyl 2-bromo-2-(diethoxyphosphoryl)-3-(imidazo[1,2-a] pyridin-3-yl)propanoate (**6d**)*

^{1}H NMR ($CDCl_3$): 1.32 (t, $^3J_{HH}$ = 7.2, P(O)$(OCH_2CH_3)_2$, 6H), 1.36 (t, $^3J_{HH}$ = 7.20, C(O)OCH_2CH_3, 3H), 3.91 (dd, $^3J_{HP}$ = 16.0, $^2J_{HH}$ = 12.4, CHHCP, 1H), 4.16–4.44 (m, 3OCH_2CH_3, CHHC, 7H), 6.95 (bt, $^3J_{HH}$ = 7.0, CH, 1H), 7.28–7.32 (m, CH, 1H), 7.69 (bd, $^3J_{HH}$ = 8.8, CH, 1H), 8.39 (d, $^3J_{HH}$ = 7.0, CH). ^{31}P NMR: 14.78. ^{13}C NMR: 13.79 (s, C(O)OCH_2CH_3), 16.22 (d, $^3J_{CP}$ = 7.95, P(O)OCH_2CH_3), 16.27 (d, $^3J_{CP}$ = 7.95, P(O)OCH_2CH_3), 29.67 (s, CH_2CP), 57.80 (d, $^1J_{CP}$ = 141.6, CP), 63.55 (s, C(O)OCH_2), 64.67 (d, $^2J_{CP}$ = 6.6, P(O)OCH_2), 65.69 (d, $^2J_{CP}$ = 5.9, P(O)OCH_2), 112.00 (s, CH), 117.45 (s, CH), 118.78 (d, $^3J_{CP}$ = 10.7, C), 124.26 (s, 2CH), 134.07 (s, CH), 145.36 (s, CH), 166.29 (s, C═O). Partially purified by preparative TLC (DCM:MeOH 16:1).

7.4. General method for hydrolysis of triesters

The ester **6a** (70.6 mg, 0.20 mmol) was dissolved in concentrated HCl (3 mL) and refluxed for 6 h. After evaporation to dryness and re-precipitation from acetone and ethanol, **7a** was obtained (36 mg) as a colourless solid (66%). Similarly obtained were **7b** (58%), **7c** (75%), **7d** (86%).

*7.4.1. 3-(Imidazo[1,2-a]pyridin-3-yl)-2-phosphonopropanoic acid (**7a**)*

^{1}H NMR (D_2O, pH 2.8): 3.31–3.45 (m, 2H), 3.57–3.66 (m, 1H), 7.49 (t, $^3J_{HH}$ = 6.8 Hz, CH, 1H), 7.74 (s, CH, 1H), 7.85–7.94 (m, 2H), 8.63 (d, $^3J_{HH}$ = 6.8 Hz, CH, 1H); ^{31}P NMR (D_2O, pH 2.8): 12.93. Anal. calcd for $C_{10}H_{11}N_2O_5P(H_2O)_{0.5}$: C 43.02%, H 4.33%, N 10.03%. Found: C 42.88%, H 4.00%, N 9.91%.

*7.4.2. 2-Fluoro-3-(imidazo[1,2-a]pyridin-3-yl)-2-phosphonopropanoic acid (**7b**)*

^{1}H NMR (D_2O, pH 2.7): 3.77–4.12 (m, 2H), 7.45 (t, $^3J_{HH}$ = 6.8 Hz, CH, 1H), 7.78 (s, CH, 1H), 7.84–7.92 (m, 2CH, 2H), 8.67 (d, $^3J_{HH}$ = 6.8, CH, 1H). ^{31}P NMR (D_2O, pH 12.3): 10.13 (d, $^2J_{PF}$ = 70.6 Hz). ^{19}F NMR (D_2O, pH 12.3): −164.5 (dd, $^2J_{PF}$ = 68.9 Hz, $^3J_{FH}$ = 41.0 Hz). Anal. calcd for $C_{10}H_{10}FN_2O_5P(H_2O)_{3.9}(C_2H_5OH)_{0.01}(C_3H_6O)_{0.02}$: C 33.63%, H 5.03%, N 7.78%. Found: C 33.99%, H 5.43%, N 7.79%.

*7.4.3. 2-Chloro-3-(imidazo[1,2-a]pyridin-3-yl)-2-phosphonopropanoic acid (**7c**)*

^{1}H NMR (D_2O, pH 2.6): 3.81 (dd, $^3J_{HP}$ = 6.4, $^2J_{HH}$ = 16.0 Hz, CH_2P, 1H), 4.24 (dd, $^3J_{HP}$ = 4.8, $^2J_{HH}$ = 16.0 Hz, CH_2P, 1H), 7.46 (dt, $^3J_{HH}$ = 6.8 Hz, $^4J_{HH}$ = 1.6, CH, 1H), 7.85–7.94 (m, 2CH, 2H), 7.87 (s, CH, 1H), 8.81 (d, $^3J_{HH}$ = 6.8 Hz, CH, 1H). ^{31}P NMR (D_2O, pH 2.6): 9.68. Anal. calcd for $C_{10}H_{10}ClN_2O_5P(H_2O)_{1.7}$: C 35.83%, H 4.03%, N 8.35%. Found: C 35.85%, H 3.74%, N 7.98%.

*7.4.4. 2-Bromo-3-(imidazo[1,2-a]pyridin-3-yl)-2-phosphonopropanoic acid (**7d**)*

^{1}H NMR (D_2O, pH 2.5): 3.86 (dd, $^3J_{HP}$ = 6.8, $^2J_{HH}$ = 16.4 Hz, CH_2P, 1H), 4.28 (dd, $^3J_{HP}$ = 5.2, $^2J_{HH}$ = 16.4 Hz, CH_2P, 1H), 7.45 (t, $^3J_{HH}$ = 7.2 Hz, CH, 1H), 7.84–7.92 (m, 2CH, 2H), 7.90 (s, CH, 1H), 8.81 (d, $^3J_{HH}$ = 6.8 Hz, CH, 1H). ^{31}P NMR (D_2O, pH 2.5): 9.68. Anal. calcd for $C_{10}H_{10}BrN_2O_5P(H_2O)_{1.5}$: C 31.94%, H 3.48%, N 7.45%. Found: C 32.08%, H 3.30%, N 7.22%.

7.5. Crystallization of (−)-1

Fractions of (−)-**1** collected in polypropylene test tubes [2] after two prep. chiral HPLC purifications were evaporated to dryness and converted into the free acid form by treatment with Dowex 50 W × 80–200 cation exchange resin (H^+ form). The fractions were collected in polypropylene test tubes, evaporated to dryness, and the yield determined by UV [2].

The resulting (−)-**1** (1.3 mg) was dissolved in water (160 μL), pH 2.5. The vial was left open in a closed jar containing acetone at RT. On the same day, a precipitate was observed. After 2d, the system was left open for complete evaporation and after an additional 4 d two crystals were harvested and subjected to X-ray diffraction analysis.

*7.6. Crystal structure determination for (−)-**1***

A specimen of $C_{10}H_{15}N_2O_8P$ approximate dimensions 0.22 mm × 0.21 mm × 0.09 mm, was used for the X-ray crystallographic analysis. The X-ray intensity data were measured on a Bruker SMART APEX CCD system equipped with a graphite monochromator and a Mo K_α sealed tube (λ = 0.71073 Å) using SMART V 5.625 (Bruker AXS, 2001). A total of 1850 frames with an exposure time of 10 s were collected. The frames were integrated with the SAINT V 6.22 program package (Bruker AXS, 2001). The integration of the data using a triclinic unit cell yielded a total of 5732 reflections, of which 4674 were independent

(completeness = 95.4%, Rint = 1.42%). The final cell constants were a = 8.1581(11) Å, b = 9.0992(12) Å, c = 9.3617(12) Å, α = 105.929(2)°, β = 97.568(2)°, and γ = 91.778(2)°. Data were corrected for absorption effects using the multi-scan method (SADABS, Bruker 2001). The calculated minimum and maximum transmission coefficients (based on crystal size) are 0.791 and 0.965.The structure was solved by direct methods and refined using the Bruker SHELXTL 5.10 Software Package (Bruker AXS, 2000), using the space group P1. The final anisotropic full-matrix least-squares refinement on F^2 with 431 variables converged at R_1 = 3.7%, for the observed data and wR_2 = 9.36% for all data.

Crystallographic data (excluding structure factors) for the structures in this paper have been deposited with the Cambridge Crystallographic Data Centre as supplementary publication no. CCDC813786. Copies of the data can be obtained, free of charge, on application to CCDC, 12 Union Road, Cambridge CB2 1EZ, UK, (fax: +44-(0)1223-336033 or e-mail: deposit@ccdc.cam.ac.uk).

Acknowledgement

This work was supported by Procter & Gamble Pharmaceuticals, Inc. and Warner Chilcott Pharmaceuticals. K.M.B. was a 2007–2009 USC WiSE Fellow.

Appendix. Supplementary material

Supplementary data associated with this article can be found, in the online version, at doi:10.1016/j.ejmech.2011.04.063.

References

[1] R.A. Baron, R. Tavare, A.C. Figueiredo, K.M. Blazewska, B.A. Kashemirov, C.E. McKenna, F.H. Ebetino, A. Taylor, M.J. Rogers, F.P. Coxon, M.C. Seabra, Phosphonocarboxylates inhibit the second geranylgeranyl addition by Rab geranylgeranyl transferase, J. Biol. Chem. 284 (2009) 6861–6868.

[2] C.E. McKenna, B.A. Kashemirov, K.M. Blazewska, I. Mallard-Favier, C.A. Stewart, J. Rojas, M.W. Lundy, F.H. Ebetino, R.A. Baron, J.E. Dunford, M.L. Kirsten, M.C. Seabra, J.L. Bala, M.S. Marma, M.J. Rogers, F.P. Coxon, Synthesis, chiral high performance liquid chromatographic resolution and enantiospecific activity of a potent new geranylgeranyl transferase inhibitor, 2-hydroxy-3-imidazo[1,2-a]pyridin-3-yl-2-phosphonopropionic acid, J. Med. Chem. 53 (2010) 3454–3464.

[3] F.P. Coxon, M.H. Helfrich, B. Larijani, M. Muzylak, J.E. Dunford, D. Marshall, A.D. McKinnon, S.A. Nesbitt, M.A. Horton, M.C. Seabra, F.H. Ebetino, M.J. Rogers, Identification of a novel phosphonocarboxylate inhibitor of Rab geranylgeranyl transferase that specifically prevents Rab prenylation in osteoclasts and macrophages, J. Biol. Chem. 276 (2001) 48213–48222.

[4] J.E. Dunford, A.A. Kwaasi, M.J. Rogers, B.L. Barnett, F.H. Ebetino, R.G.G. Russell, U. Oppermann, K.L. Kavanagh, Structure–activity relationships among the nitrogen containing bisphosphonates in clinical use and other analogues: time-dependent inhibition of human farnesyl pyrophosphate synthase, J. Med. Chem. 51 (2008) 2187–2195.

[5] M.S. Marma, Z.D. Xia, C. Stewart, F. Coxon, J.E. Dunford, R. Baron, B.A. Kashemirov, F.H. Ebetino, J.T. Triffitt, R.G.G. Russell, C.E. McKenna, Synthesis and biological evaluation of alpha-halogenated bisphosphonate and phosphonocarboxylate analogues of risedronate, J. Med. Chem. 50 (2007) 5967–5975.

[6] F.P. Coxon, F.H. Ebetino, E.H. Mules, M.C. Seabra, C.E. McKenna, M.J. Rogers, Phosphonocarboxylate inhibitors of Rab geranylgeranyl transferase disrupt the prenylation and membrane localization of Rab proteins in osteoclasts in vitro and in vivo, Bone 37 (2005) 349–358.

[7] K.W. Cheng, J.P. Lahad, J.W. Gray, G.B. Mills, Emerging role of RAB GTPases in cancer and human disease, Cancer Res. 65 (2005) 2516–2519.

[8] S. Boissier, M. Ferreras, O. Peyruchaud, S. Magnetto, F.H. Ebetino, M. Colombel, P. Delmas, J.-M. Delaisse, P. Clezardin, Bisphosphonates inhibit breast and prostate carcinoma cell invasion, an early event in the formation of bone metastases, Cancer Res. 60 (2000) 2949–2954.

[9] A.J. Roelofs, P.A. Hulley, A. Meijer, F.H. Ebetino, R. Graham, G. Russell, C.M. Shipman, Selective inhibition of Rab prenylation by a phosphonocarboxylate analogue of risedronate induces apoptosis, but not S-phase arrest, in human myeloma cells, Int. J. Cancer 119 (2006) 1254–1261.

[10] P.G.J. Fournier, F. Dauhine, M.W. Lundy, M.J. Rogers, F.H. Ebetino, P. Clezardin, Lowering bone mineral affinity of bisphosphonates as a therapeutic strategy to optimize skeletal tumor growth inhibition in vivo, Cancer Res. 68 (2008) 8945–8953.

[11] X.L. Tian, R.U. Jin, A.J. Bredemeyer, E.J. Oates, K.M. Blazewska, C.E. McKenna, J.C. Mills, RAB26 and RAB3D are direct transcriptional targets of MIST1 that regulate exocrine granule maturation, Mol. Cell. Biol. 30 (2010) 1269–1284.

[12] A.J. Roelofs, A. Boyde, M.W. Lundy, C.E. McKenna, K. Blazewska, S.T. Sun, B.A. Kashemirov, R.G.G. Russell, F.H. Ebetino, M.J. Rogers, F.P. Coxon, Bone mineral affinity influences the distribution of a bisphosphonate and a lower affinity analogue in vivo, Bone 44 (2009) S430–S431.

[13] K.T. Tan, E. Guiu-Rozas, R.S. Bon, Z. Guo, C. Delon, S. Wetzel, S. Arndt, K. Alexandrov, H. Waldmann, R.S. Goody, Y.W. Wu, W. Blankenfeldt, Design, synthesis, and characterization of peptide-based Rab geranylgeranyl transferase inhibitors, J. Med. Chem. 52 (2009) 8025–8037.

[14] Z. Guo, Y.W. Wu, D. Das, C. Delon, J. Cramer, S. Yu, S. Thuns, N. Lupilova, H. Waldmann, L. Brunsveld, R.S. Goody, K. Alexandrov, W. Blankenfeldt, Structures of RabGGTase-substrate/product complexes provide insights into the evolution of protein prenylation, EMBO J. 27 (2008) 2444–2456.

[15] A preliminary account of part of this work has been presented: K.M. Blazewska, B.A. Kashemirov, C.A. Stewart, F.P. Coxon, R. Baron, M.J. Rogers, M.C. Seabra, F.H. Ebetino, C.E. McKenna. Synthesis and biological studies on desoxy- and -halogenated phosphonocarboxylate analogs of minodronate. 42nd Western Regional Meeting of the American Chemical Society. Las Vegas, NV. September 23–27, 2008.

[16] O. Trott, A.J. Olson, Software news and update AutoDock Vina: improving the speed and accuracy of docking with a new scoring function, efficient optimization, and multithreading, J. Comput. Biol. 31 (2010) 455–461.

[17] P.T. Lang, S.R. Brozell, S. Mukherjee, E.F. Pettersen, E.C. Meng, V. Thomas, R.C. Rizzo, D.A. Case, T.L. James, I.D. Kuntz, DOCK 6: combining techniques to model RNA-small molecule complexes, RNA 15 (2009) 1219–1230.

[18] S.B. Long, P.J. Casey, L.S. Beese, Reaction path of protein farnesyltransferase at atomic resolution, Nature 419 (2002) 645–650.

[19] K. Ohno, K. Mori, M. Orita, M. Takeuchi, Computational insights into binding of bisphosphates to farnesyl pyrophosphate synthase, Curr. Med. Chem. 18 (2011) 220–233.

[20] D. Parker, Nmr Determination of enantiomeric purity, Chem. Rev. 91 (1991) 1441–1457.

[21] J.M. Seco, E. Quinoa, R. Riguera, The assignment of absolute configuration by NMR, Chem. Rev. 104 (2004) 17–117.

[22] K.M. Blazewska, T. Gajda, Assignment of the absolute configuration of hydroxy- and aminophosphonates by NMR spectroscopy, Tetrahedron: Asymmetry 20 (2009) 1337–1361.

[23] R. Hulst, R.M. Kellogg, B.L. Feringa, New methodologies for enantiomeric excess (ee) determination based on phosphorus NMR, J. Royal Neth. Chem. Soc. 114 (1995) 115–138.

[24] K. Blazewska, T. Gajda, (S)-Naproxen (R) and (S)-Ibuprofen (R) chlorides – convenient chemical derivatizing agents for the determination of the enantiomeric excess of hydroxy and aminophosphonates by P-31 NMR, Tetrahedron: Asymmetry 13 (2002) 671–674.

[25] L. Berlicki, E. Rudzinska, P. Kafarski, Enantiodifferentiation of aminophosphonic and aminophosphinic acids with alpha- and beta-cyclodextrins, Tetrahedron: Asymmetry 14 (2003) 1535–1539.

[26] A.W. Schuttelkopf, D.M.F. van Aalten, PRODRG: a tool for high-throughput crystallography of protein-ligand complexes, Acta Crystallogr. Sect. D Biol. Crystallogr. 60 (2004) 1355–1363.

[27] L. Almirante, A. Mugnaini, N. De Toma, A. Gamba, W. Murmann, J. Hidalgo, Imidazole derivatives. IV. Synthesis and pharmacologic activity of oxygenated derivatives of imidazo[1,2-a]pyridine, J. Med. Chem. 13 (1970) 1048–1051.

[28] A. Gueiffier, M. Lhassani, A. Elhakmaoui, R. Snoeck, G. Andrei, O. Chavignon, J.C. Teulade, A. Kerbal, E.M. Essassi, J.C. Debouzy, M. Witvrouw, Y. Blache, J. Balzarini, E. DeClercq, J.P. Chapat, Synthesis of acyclo-C-nucleosides in the imidazo[1,2-a]pyridine and pyrimidine series as antiviral agents, J. Med. Chem. 39 (1996) 2856–2859.